



# A side-edge frame dual-band eight-element MIMO antenna array for 5G handset

cambridge.org/mrf

Mahsa Zabetiakmal , Gholamreza Moradi and Ayaz Ghorbani 

Department of Electrical Engineering, Amirkabir University of Technology, Tehran, Iran

## Research Paper

**Cite this article:** Zabetiakmal M, Moradi G, Ghorbani A (2022). A side-edge frame dual-band eight-element MIMO antenna array for 5G handset. *International Journal of Microwave and Wireless Technologies* **14**, 1119–1129. <https://doi.org/10.1017/S1759078721001446>

Received: 25 May 2021

Revised: 14 September 2021

Accepted: 18 September 2021

First published online: 14 October 2021

### Key words:

Dual-band; 5G communication; MIMO antenna; mobile phone; side-edge design

### Author for correspondence:

Mahsa zabetiakmal, E-mail: [zabeti24@aut.ac.ir](mailto:zabeti24@aut.ac.ir)

## Abstract

In this paper, a dual-band  $8 \times 8$  multi-input multi-output (MIMO) array antenna operating in 3.5 GHz band (3400–3600 MHz) and 5.5 GHz band (5150–5925 MHz) for 5G mobile handset is presented. The proposed hybrid antenna includes a comb-shaped monopole and an L-shaped open slot antenna which are symmetrically located on the inner surface of the side-edge frame of smartphone. Pattern diversity is achieved that can mitigate envelope correlation coefficients (ECCs) and improve the MIMO system performances. The prototype of proposed dual-band eight-element MIMO antenna is fabricated and experimentally measured. The results show that isolation  $<-10$  and  $<-15$  dB, respectively in the lower band and high band without any additional decoupling element are achieved and the desired bands are satisfied under the condition of  $-6$  dB impedance matching. Moreover, the essential parameters for evaluation of the MIMO system performance such as the ECC, mean effective gain (MEG), and ergodic channel capacity are calculated. Furthermore, the influence of user's hand on the radiation characteristics of proposed MIMO antenna are also investigated and discussed. Based on the result, the proposed MIMO antenna is a good candidate for use in future 5G applications.

## Introduction

The multi-input multi-output (MIMO) technology increases channel capacity, spectral efficiency, and reliability link without the need for additional bandwidth and power [1–3]. Because of these advantages, it has become a major technology for 5G communications. At the World Radio Communication Conference 2015 (WRC-2015), the 3.5 GHz band (3400–3600 MHz) has been introduced as one of the 5G mobile phone frequency bands [4]. The 5.5 GHz band (5150–5925 MHz) is also considered to further support sub-6 GHz frequency band.

Due to the compact volume for inserting a large number of antennas into mobile phone and strong mutual coupling between its single antenna elements and good efficiency, how to achieve high isolation and low correlation coefficient between them is a major challenge in MIMO antenna design. Several decoupling techniques have been presented such as neutralization line and ground slot [5–7], decoupling network [8], orthogonality dual-polarized antenna [9–11], pattern diversity [12], multimode decoupling [13]. Utilizing these techniques, in addition to the complexity of structure, reduces the total efficiency of antenna. Therefore, there is always a trade off between the increase of order of MIMO, reduction of coupling and good efficiency.

In recent years, several MIMO antennas have been reported [14–19]. In [14], an 8-element MIMO which is composed of folded monopole and gap-coupled loop antenna that covers 3.4–3.6 GHz and 4.8–5.1 GHz has been presented and isolation better than 11.5 dB by using neutralization line and efficiency better than 40% are achieved. In [15], an  $8 \times 8$  MIMO antenna including an L-shaped open slot and a U-shaped monopole antenna are investigated that covers 3.5 and 5 GHz band. An isolation better than 12 dB, total efficiency more than 50% and,  $ECC < 0.1$  are achieved. Nevertheless, in the both designs in [14] and [15] which consider multi-band operation, the high isolation and enough total efficiency have not been achieved. In [16], self-isolated antenna elements for MIMO array have been presented, which are one T-shaped feeding element and two identical L-shaped elements and therefore an isolation better than 20 dB has been obtained. In [17] a single-band  $8 \times 8$  MIMO consist of two asymmetrically mirrored gap-coupled loop antennas as a compact building block of antenna array operating at 3.5 GHz band has been proposed. The total size of the proposed building block was  $7 \text{ mm} \times 10 \text{ mm}$ , which is very compact for mobile phone application.

An isolation better than 10 dB is obtained without any external decoupling structure. The high isolation MIMO array consists of two types of four antenna arrays (U-shaped and L-shaped coupled-fed loop elements) that is presented in [5] that covers the desired band 3.3–3.6 GHz. The isolations 15 dB are enhanced by combining the inverted-I ground slots with neutralization line structure. Another design of dual-polarized eight element MIMO antenna is proposed in [18] that contains a compact square-ring slot antenna fed by

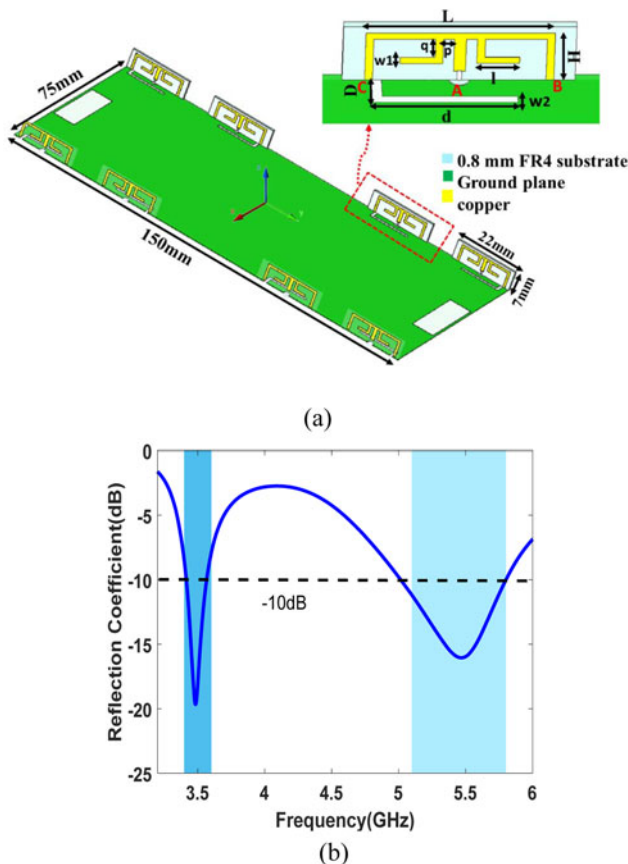


**Fig. 1.** (a) The geometry of the proposed eight elements and (b) the simulated reflection coefficient of single element.

rectangular microstrip-line. A pair of circular ring/open-ended parasitic structure has been employed across the ring slot to reduce the mutual coupling between two microstrip feeding ports up to 17 dB. However, high isolation and good MIMO performance is achieved, multi-band operation antenna which is important in the mobile phone communication has not been implemented in [5, 16–18].

In this paper an 8-element MIMO array operating in 3.5 GHz band (3400–3600 MHz) and 5.5 GHz band (5150–5925 MHz) is presented. By using coupled feeding structure in the array, dual-band antenna is achieved. The proposed antenna consists of L-shaped open slots and comb-shaped monopole antenna, which are located on the inner surface of the side-edge frame of mobile phone. Simulation results of the proposed antenna have demonstrated that good isolation ( $<10$  and  $<15$  dB) in lower and high band is achieved with high total efficiency (more than 70%) and  $ECC < 0.15$ . Due to mirrored arrangement design of MIMO antenna elements, pattern diversity is achieved that improves the performance of MIMO system by mitigating envelope correlation coefficients (ECCs). Furthermore, the proposed MIMO antenna provides a desirable isolation with good radiation characteristics in vicinity of user's hand.

## The proposed antenna

### Antenna structure

The detailed and physical dimensions of the proposed eight element MIMO array are displayed in Fig. 1(a). The antenna elements

are placed symmetrically on the inner surface of the frame of the mobile phone. The mobile phone frames have thickness of 0.8 mm and height of 7 mm that are placed perpendicularly on the PCB board. The size of the substrate is 150 and 75 mm which is a typical size of 5.5-inch smartphone. FR4 substrate (relative permittivity = 4.4, loss tangent = 0.02) is considered as the printed circuit board (PCB) of system and side-edge frame. Each dual-band antenna consists of an L-shaped open slot antenna on the ground and comb-shaped monopole antenna. The monopoles are fed by the  $50 \Omega$  microstrip line that is connected by a  $50 \Omega$  SMA connector at point A. The monopole is connected to the ground plane at points B and C.

### Parametric analysis

Figure 1(b) shows the simulated reflection coefficient of single element antenna. It is observed that the two desired bands are fully covered under the condition of  $-10$  dB return loss. In this design, the comb-shaped monopole antenna and the L-shaped open slot antenna are used to generate the 5.5 and 3.5 GHz resonant, respectively. To further verify the resonant mode of the two proposed antenna, the simulated surface current and E-field distributions at 3.5 and 5.5 GHz are depicted in Figs 2(a) and 2(b). At 3.5 GHz, as shown in Fig. 2(a) it can be easily seen that strong surface current distributions are mainly concentrated on the closed end of the slot, showing the L-shaped open slot antenna operates at the fundamental quarter-wavelength resonant mode. Hence, the first resonance is determined by the length of L-shaped open slot antenna ( $d$ ), as shown in Fig. 3(a). It is also seen in Fig. 2(b), that there are two current nulls along monopole, which indicates the first higher order mode at high band. Similarly, for H and L fixed, impedance matching and resonant frequency of high band can be fine-tuned by parameter  $l$ , as shown in Fig. 3(b). It is also observed that the two modes can be tuned separately. The optimized parameters of the proposed single antenna are displayed in Table 1.

### Array design

In dual-element antenna array, there are two kinds of arrangement, namely mirrored and shifted configurations that is illustrated in Figs 4(a) and 4(b), respectively. The simulated transmission coefficients of two configurations with different space between them ( $d_{12}$ ), are shown in Fig. 5. It is observed that in the mirrored case, transmission coefficient  $S_{21}$  is less than  $-15$  and  $-20$  dB in the low band and high band for  $d_{12} = 14$  mm, while in shifted case, the same  $S_{21}$  value is not achieved even for larger  $d_{12}$ . Therefore, we will use the mirrored configuration for designing eight-element MIMO antenna array.

## Eight antenna MIMO array

### Array configuration and performances

Two different arrangements of  $8 \times 8$  MIMO antenna array are presented namely, cases I and II as illustrated in Fig. 6. In case I, all of the elements are symmetrically located on the two-long edges of smartphone, but in the case II, four elements are located on the two long edges and four other antennas on the top and bottom edges. Based on the result of [19], the configuration of case I is considered hereafter. The 3D radiation patterns of Ant1-Ant4 at 3.5 and 5.5 GHz are shown in Figs 7(a) and 7(b),

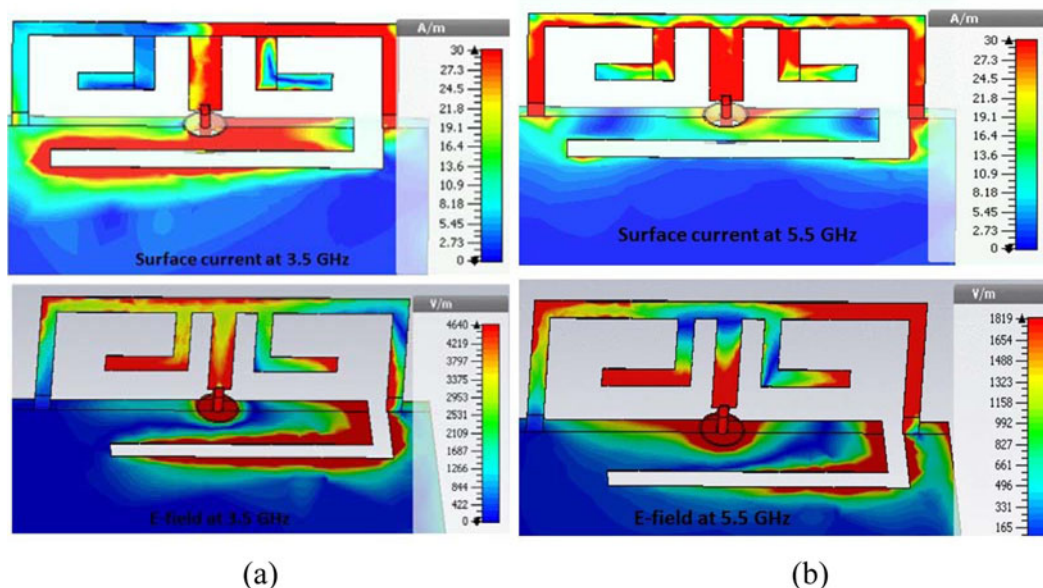


Fig. 2. Simulated surface current and E-field distributions at (a) 3.5 GHz and (b) 5.5 GHz.

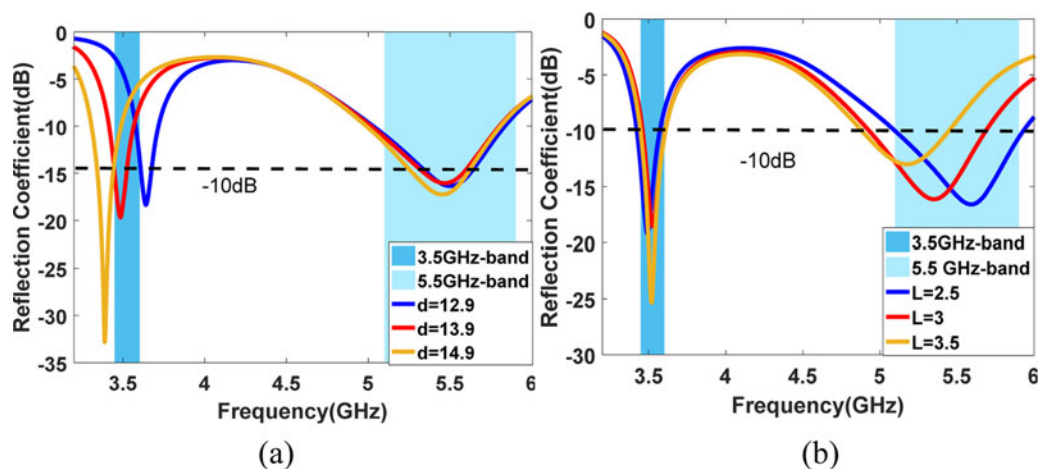


Fig. 3. Simulated reflection coefficient for different (a) length of slots and (b) length of monopoles.

respectively. It can be seen that each side of the space has been fully covered.

Thus, the proposed MIMO antenna array presents good radiation coverage which makes it more appropriate to be used in future mobile phones. Also, it can be observed that the maximum radiating orientations of antenna are in different directions, hence, diversity pattern is achieved which, is an advantage for good MIMO performance. Figure 8 depicts the simulated total efficiency. It is seen that, the total efficiencies are better than 60 and 80% in the 3.5 and 5.5 GHz band, respectively.

### Measurement and result

A prototype of the proposed MIMO antenna array was fabricated and tested. Each element was connected to a 50- $\Omega$  SMA connector by RF coaxial cable at the corresponding feeding point to the back of system circuit board. It should be noted that, due

to the proximity of feeding point to the L-shaped slot and the limitations of fabrication, the clearance width of L-shaped open slot antenna was considered  $d = 3$  mm. The photo of fabricated MIMO antenna array, and its front, side and back view are illustrated in Fig. 9. The measured results were obtained when one antenna element is excited and the other elements, which are not under test, terminated to 50- $\Omega$  loads.

### S-Parameters

The simulated and measured  $S$  parameters are shown in Fig. 10. Due to the symmetrical structure, only the results of the Ant 1–4 are given. It is observed that, the measured  $S_{11}$ ,  $S_{22}$ ,  $S_{33}$  and  $S_{44}$  are smaller than  $-6$  dB in the two desired frequency band, and the measured isolations between two adjacent ports ( $S_{12}$ ,  $S_{23}$ ,  $S_{34}$ , and  $S_{24}$ ) are better than 11.5 and 15 dB whit in the low band and high band, respectively. Therefore, there are good agreement

**Table 1** Optimized parameters of antenna.

Parameters	Value (mm)
<i>L</i>	19
<i>H</i>	6.2
<i>l</i>	2.75
<i>W<sub>1</sub></i>	0.8
<i>q</i>	4
<i>p</i>	2
<i>D</i>	3
<i>d</i>	13
<i>W<sub>2</sub></i>	1

between the simulated and measured *S* parameters and the little differences are due to the connector and fabrication losses.

**Radiation pattern**

The measured and simulated total realized gain patterns of Ant1–4 in the xoy plane at two different frequency 3.5 and 5.5 GHz are illustrated in Figs 11 and 12, respectively. Although in some direction the measured pattern has not tracked the corresponding simulation result, the overall trend of the two results are similar and the slight difference possibly is due to the test environment

errors and other external disturbances. Also, it is observed that Ant1–Ant4 have strong radiation in the  $\varphi = 315^\circ$ ,  $\varphi = 210^\circ$ ,  $\varphi = 180^\circ$ , and  $\varphi = 65^\circ$ , respectively, in the 3.5 GHz frequency. As shown in Fig. 12, in the 5.5 GHz frequency, maximum radiation is oriented in at the  $\varphi = 330^\circ$ ,  $\varphi = 90^\circ$ ,  $\varphi = 270^\circ$ , and  $\varphi = 30^\circ$ , respectively. In conclusion, because of difference in the maximum radiating orientations, diversity pattern is achieved which, is an advantage for good MIMO performance.

**MIMO performance**

Beside the other radiation performance of antenna, it is important to investigate ECC, mean effective gain (MEG), and channel capacity to evaluate diversity performance of the proposed MIMO antenna. The ECC values are calculated from measured complex radiation far field of antenna by formula explained in [20] and are depicted in Fig. 13. It is observed that the calculated ECC values were smaller than 0.15 which is better than its acceptable threshold.

The MEG of Ant1–4 under propagation conditions Gaussian/uniform (XPR = 5 dB,  $m_v = 10^\circ$ ,  $m_H = 10^\circ$ ,  $\sigma_v = 15^\circ$ ,  $\sigma_H = 15^\circ$ ) [20] were computed directly from CST by the simulated 3D far-field radiation patterns. Then, branch power ratio (*k*) was calculated for the two antennas by following formula [21]:

$$k_{i,j} = \min\left(\frac{MEG_i}{MEG_j}, \frac{MEG_j}{MEG_i}\right) \tag{1}$$

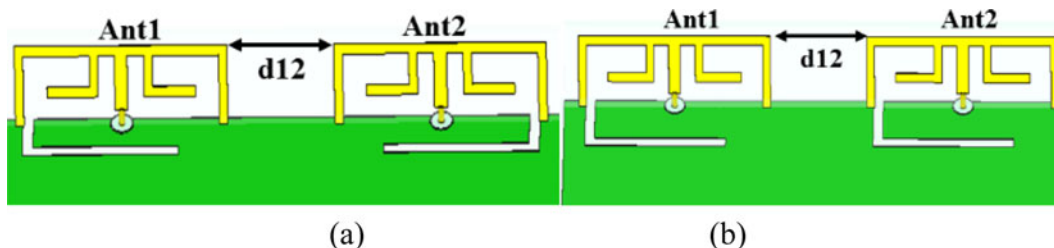


**Fig. 4.** Two arrangement of dual-element array (a) mirrored and (b) shifted configuration.

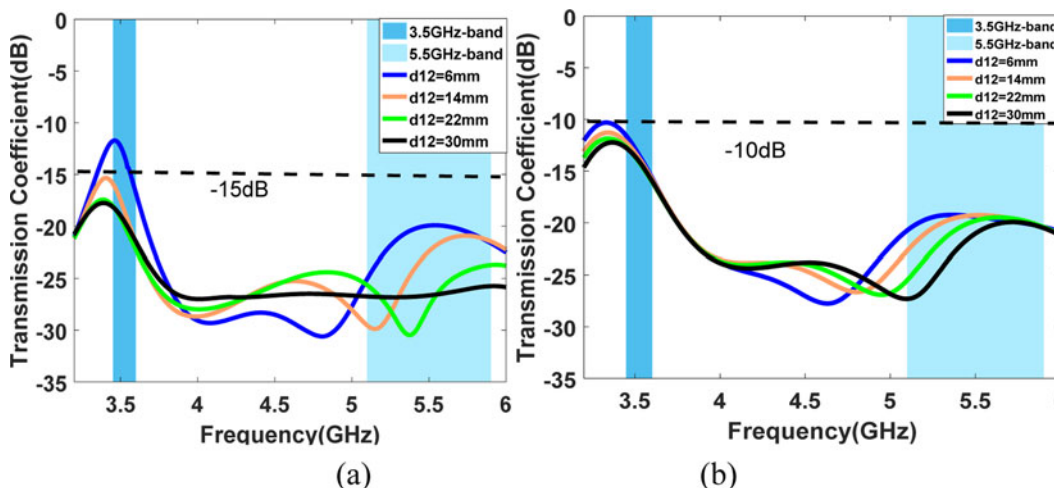


**Fig. 5.** Simulated transmission coefficient of two configuration (a) mirrored and (b) shifted.

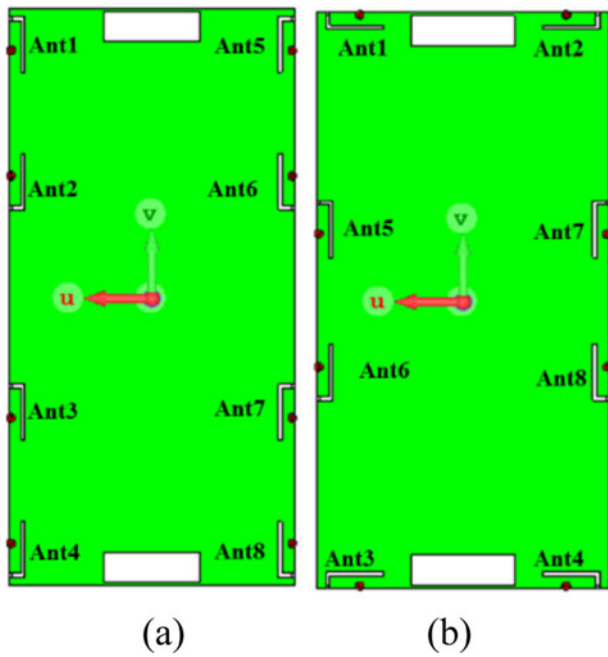


Fig. 6. Two different configurations of eight-elements of MIMO antennas array (a) case I and (b) case II.

The calculated MEG and branch power ratio ( $k$ ) of Ant1-4 are shown in Table 2. It is observed that  $k$  is more than  $-3$  dB which is essential to obtain the maximum diversity gain and avoid significant loss in the diversity performance of the MIMO antenna system [21].

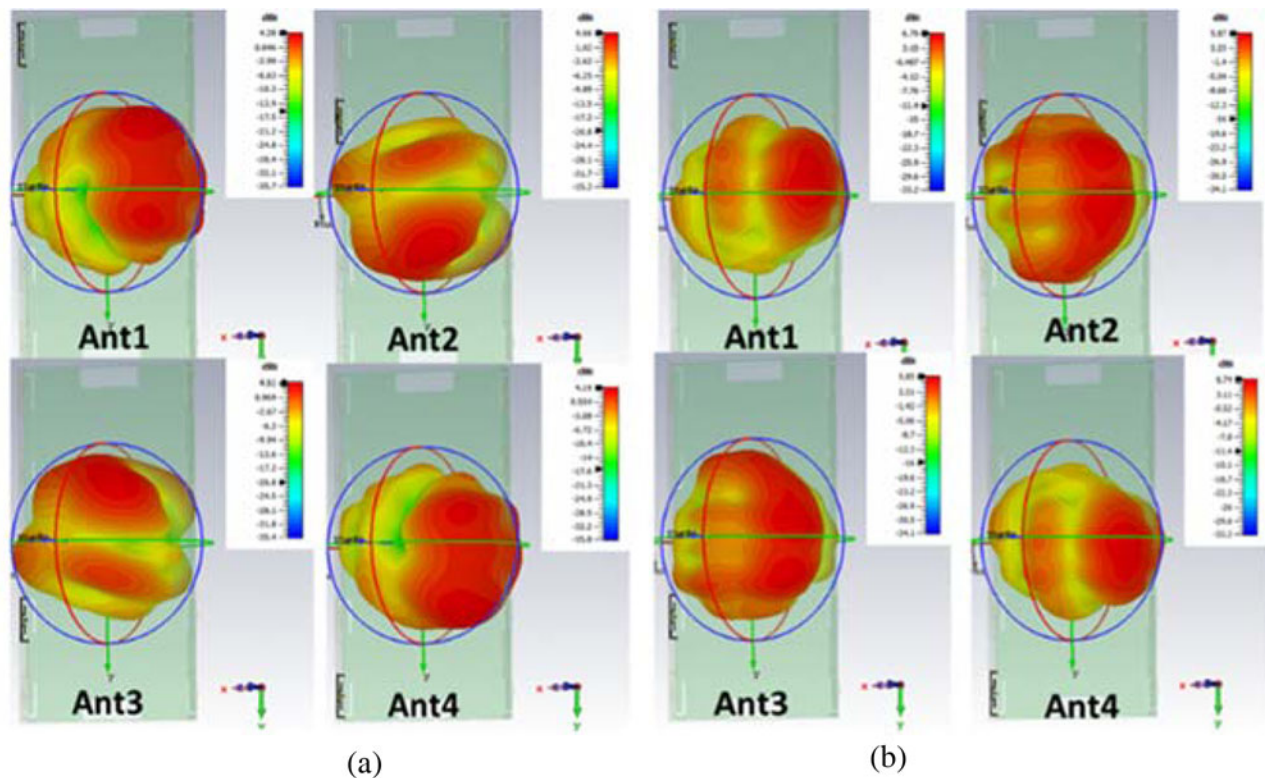


Fig. 7. Simulated 3D radiation pattern of Ant1-4 at (a) 3.5 GHz and (b) 5.5 GHz.

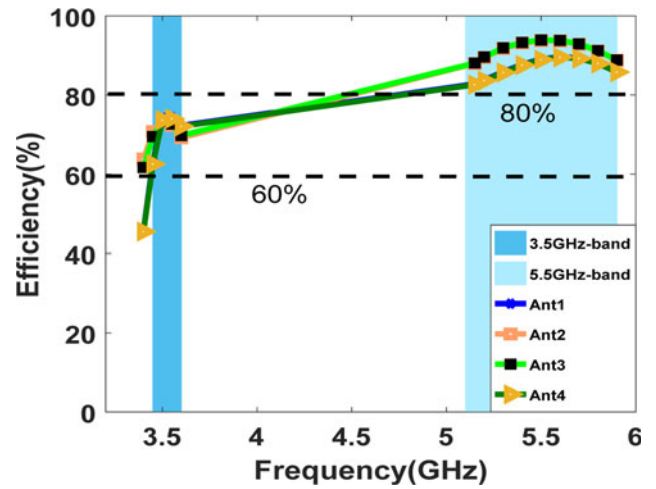


Fig. 8. Simulated total efficiency of Ant1-4.

If the transmitter does not know the channel state information (CSI) and the transmit power is equally allocated to every transmit antenna, the ergodic channel capacity can be achieved by the formula given in [22]

$$C = E \left\{ \log_2 \det \left( I + \eta \frac{SNR}{N} HH^H \right) \right\} \quad (2)$$

where  $I$  is the identity matrix, SNR denotes the mean SNR,  $N$  is the rank of the matrix  $HH^T$ ,  $H$  is the channel matrix, and  $H^H$  denotes the Hermitian transpose of matrix. The channel matrix  $H$  is calculated by the Kronecker channel model [23].

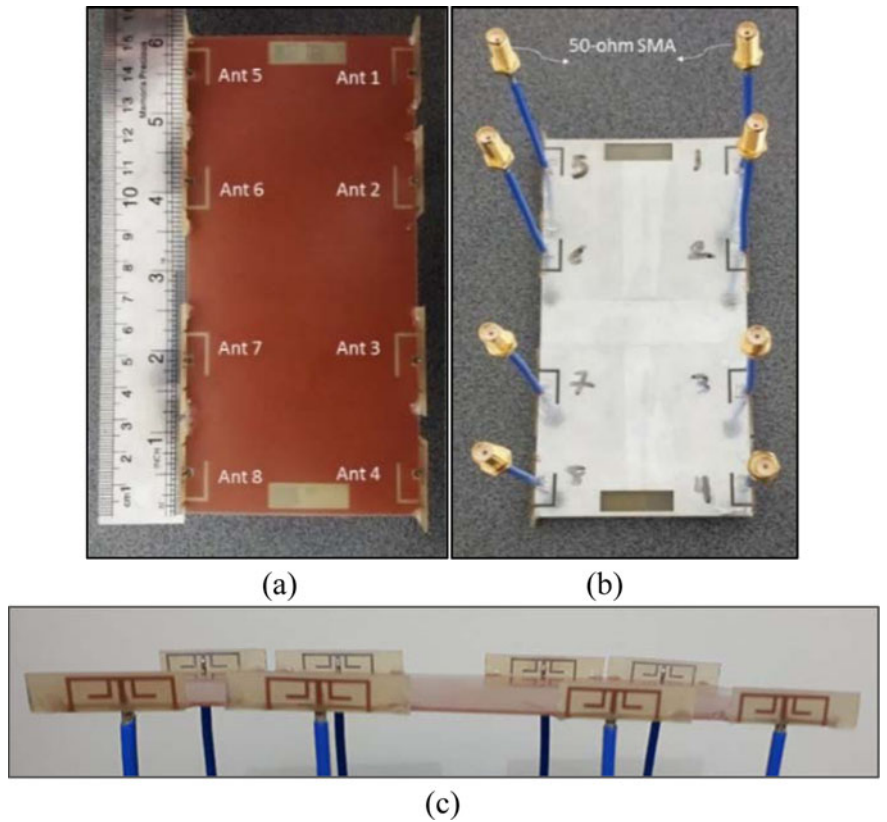


Fig. 9. Fabricated of the proposed MIMO antenna array (a) top view, (b) bottom view and (c) side view.

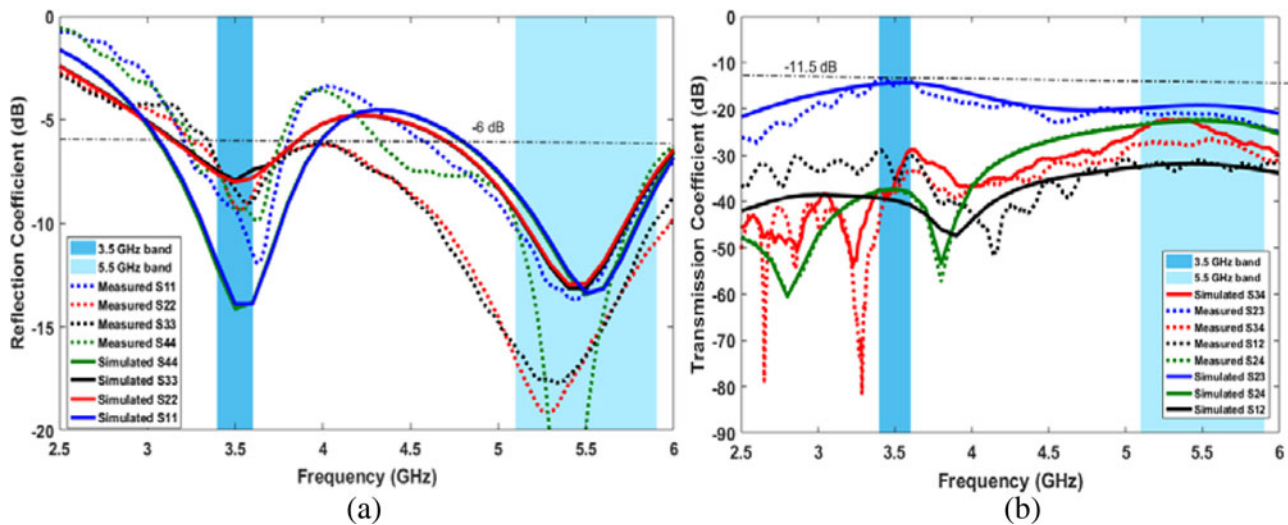


Fig. 10. Simulated and measured results of (a) reflection coefficient and (b) transmission coefficient.

Using this model, the complex channel matrix  $H$  can be expressed as

$$H = \Phi_R^{1/2} H_w \Phi_T^{1/2} \quad (3)$$

where  $\Phi_R$  and  $\Phi_T$  are the receive and transmit antenna correlation matrix, respectively and  $\{.\}^{1/2}$  denotes the matrix square root.  $H_w$  is the white channel matrix that describes the properties of the propagation scenario. When an independent and identically

distributed (i.i.d.) Rayleigh fading channel is assumed, the entries of  $H_w$  are zero-mean circularly symmetric complex Gaussian random variables. It should be noted that the impact of the total efficiency on the antenna correlation matrix is considered here, as explained in [24]

$$\begin{aligned} \Phi_R &= \eta_r^{1/2} \Psi_R^{1/2} \eta_r^{1/2} \\ \Phi_T &= \eta_t^{1/2} \Psi_T^{1/2} \eta_t^{1/2} \end{aligned} \quad (4)$$

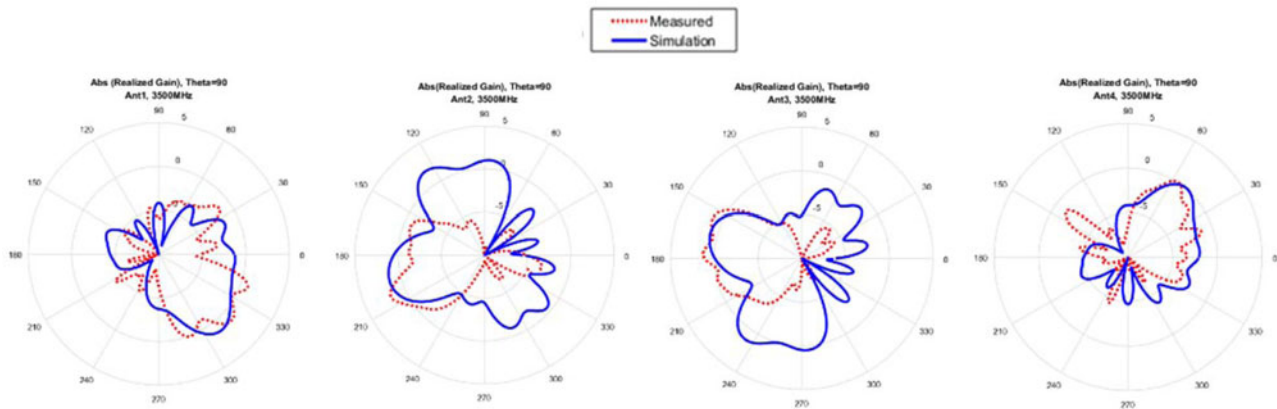


Fig. 11. Simulated and measured total realized gain pattern Ant1-4 at 3.5 GHz.

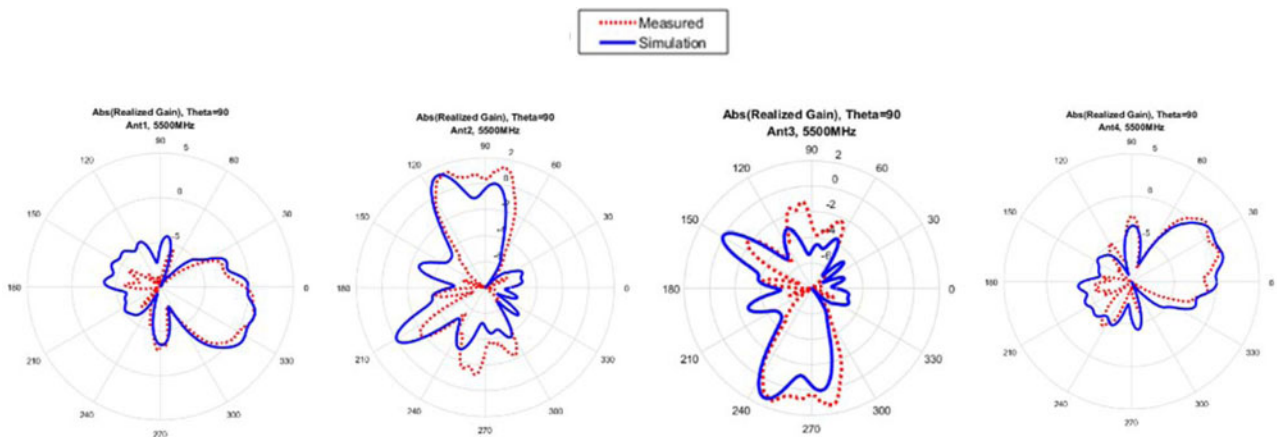


Fig. 12. Simulated and measured total realized gain pattern Ant1-4 at 5.5 GHz.

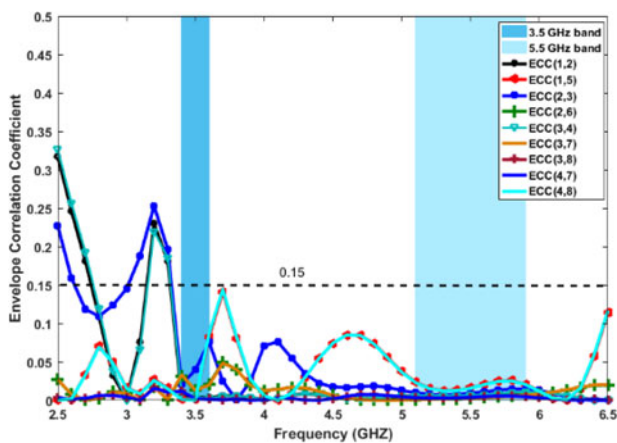


Fig. 13. Simulated ECC values between some adjacent elements.

where  $\eta_r$  and  $\eta_t$  are the receive and transmit diagonal matrices containing the total efficiencies of the receive and transmit antenna elements. By assuming all the antenna elements at transmitter are uncorrelated, i.e., zero-correlation coefficient, the  $(i, j)^{th}$

Table 2 MEG and branch power ratio ( $K$ ).

Parameters (GHz)	MEG1 (dB)	MEG2 (dB)	MEG3 (dB)	MEG4 (dB)
3.5	-4.33	-4.69	-4.65	-4.36
5.5	-2.62	-1.76	-1.87	-2.62
	$K_{12}$	$K_{23}$	$K_{34}$	$K_{24}$
3.5	-0.36	-0.04	-0.29	-0.33
5.5	-0.86	-0.11	-0.75	-0.86

entry of  $\Psi_R$  is calculated by [25]

$$\Psi_R^{(i,j)} = \frac{\mu_{ij}}{\sqrt{\mu_{ii}\mu_{jj}}} \tag{5}$$

$$\mu_{ij} = \int E\{[A_i(\Omega)h(\Omega)][A_j^*(\Omega)h^*(\Omega)]d\Omega\}$$

where  $A_i(\Omega)$  and  $A_j(\Omega)$  represent the field patterns of antenna element  $i$  and  $j$ ,  $h(\Omega)$  represent incoming wave,  $\{ \}^*$  denotes

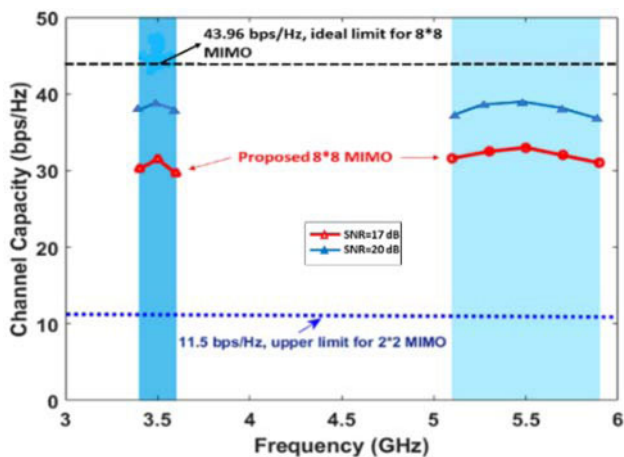


Fig. 14. Calculated channel capacity from measured result.

conjugate operation,  $E\{ \}$  represents expectation. The mobile wireless environment defined in [26] has a series of reasonable assumptions: the fading envelope being Rayleigh distributed, the incoming wave arriving in horizontal plane only, the incoming wave's orthogonal polarizations being uncorrelated, the individual polarizations being spatially uncorrelated, and finally the time-averaged power density per steradian being constant. Based on these approximations and the derivation in [24], can be written as

$$\mu_{ij} = \int_0^{2\pi} \left[ \Gamma A_{i\theta} \left( \frac{\pi}{2}, \phi \right) A_{j\theta}^* \left( \frac{\pi}{2}, \phi \right) + A_{i\phi} \left( \frac{\pi}{2}, \phi \right) A_{j\phi}^* \left( \frac{\pi}{2}, \phi \right) \right] d\phi \tag{6}$$

where  $\Gamma$  is the cross-polarization discrimination (XPD) of the incoming wave, that, in this paper is set to 0 dB. As shown in Fig. 14, the channel capacity is achieved by assuming the

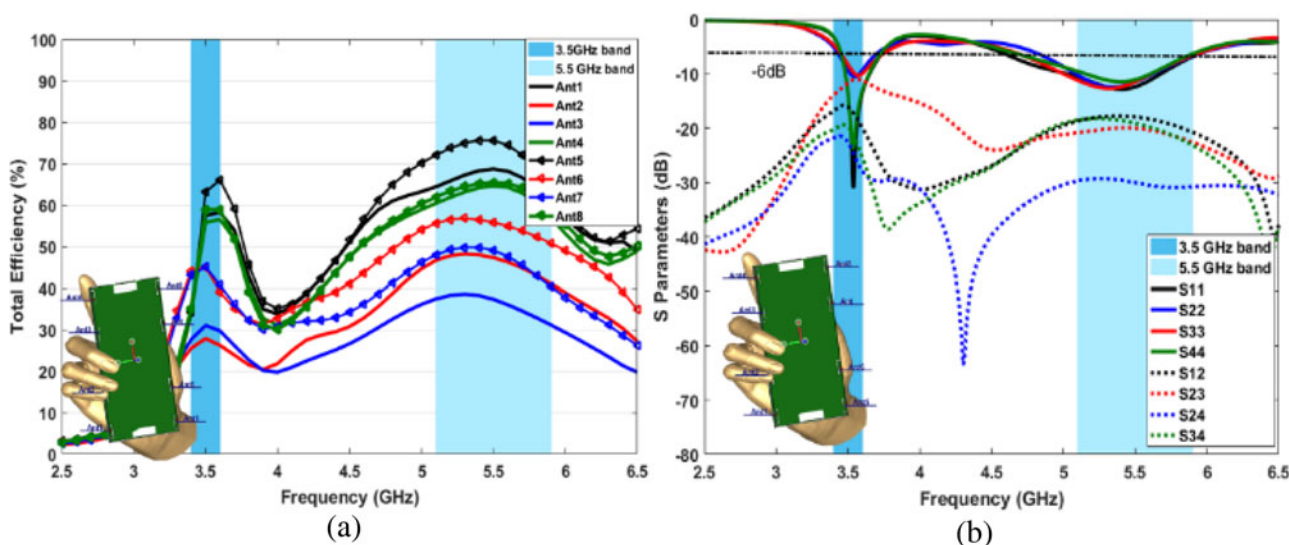


Fig. 15. Simulated (a) total efficiency and (b) S-parameters of the proposed MIMO antenna array at data mode usage.

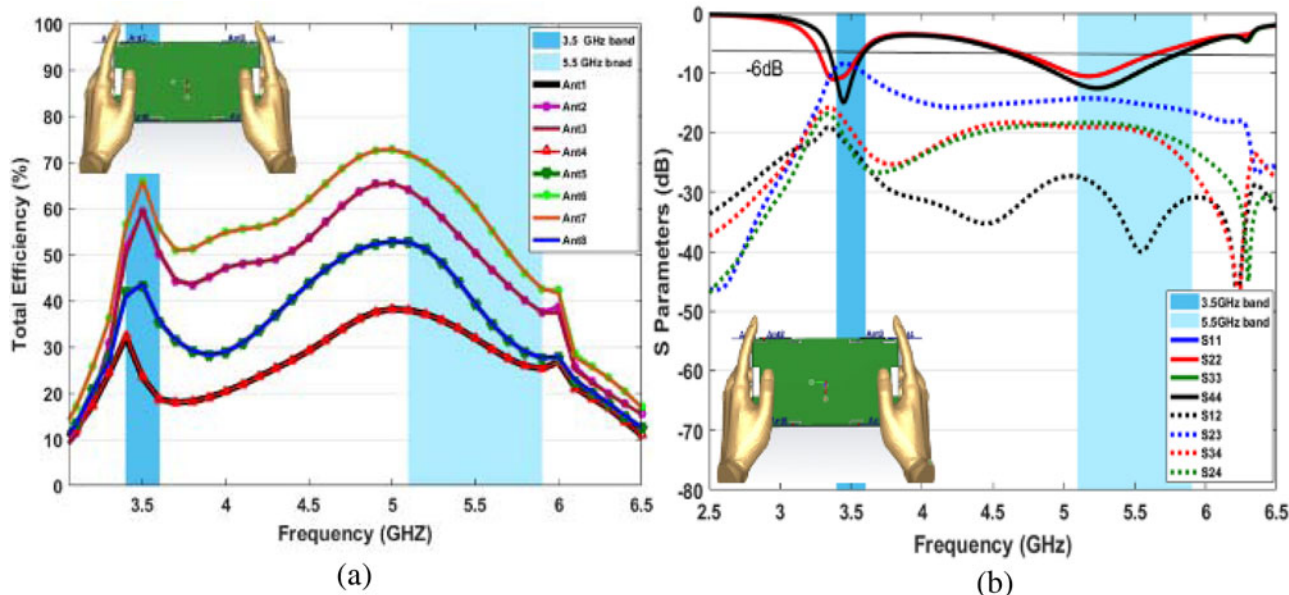


Fig. 16. Simulated (a) total efficiency and (b) S-parameters of proposed MIMO antenna array at read mode usage.



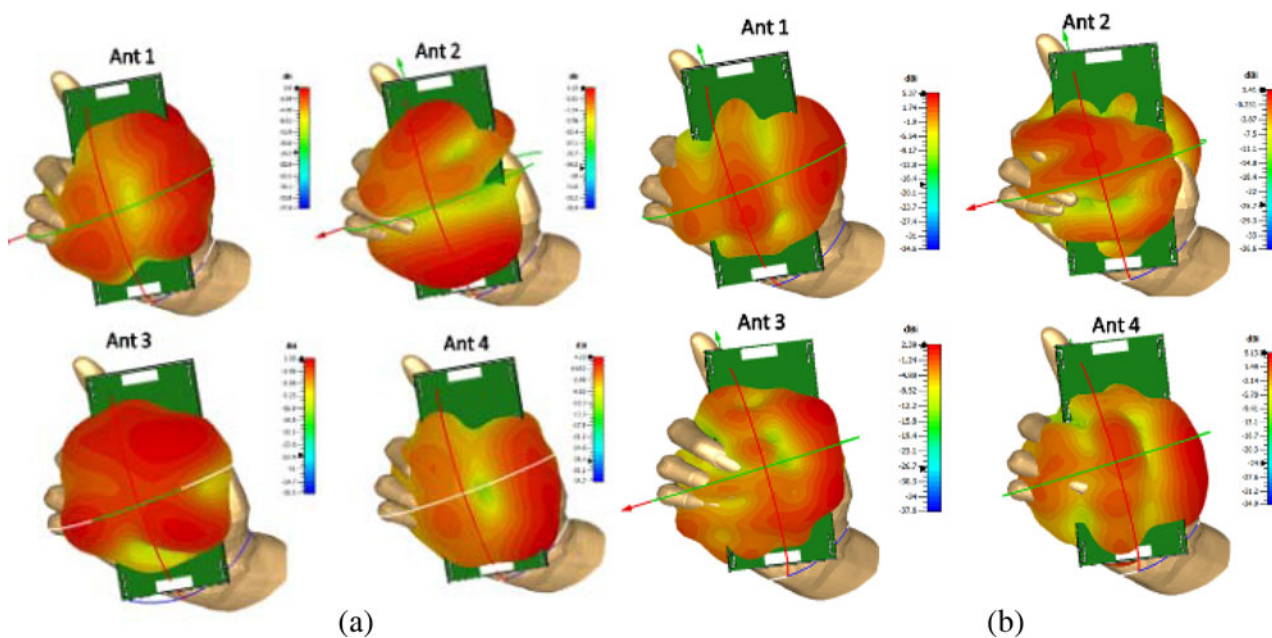


Fig. 17. Simulated 3D radiation pattern of proposed MIMO antenna array in DM usage at (a) 3.5 GHz and (b) 5.5 GHz.

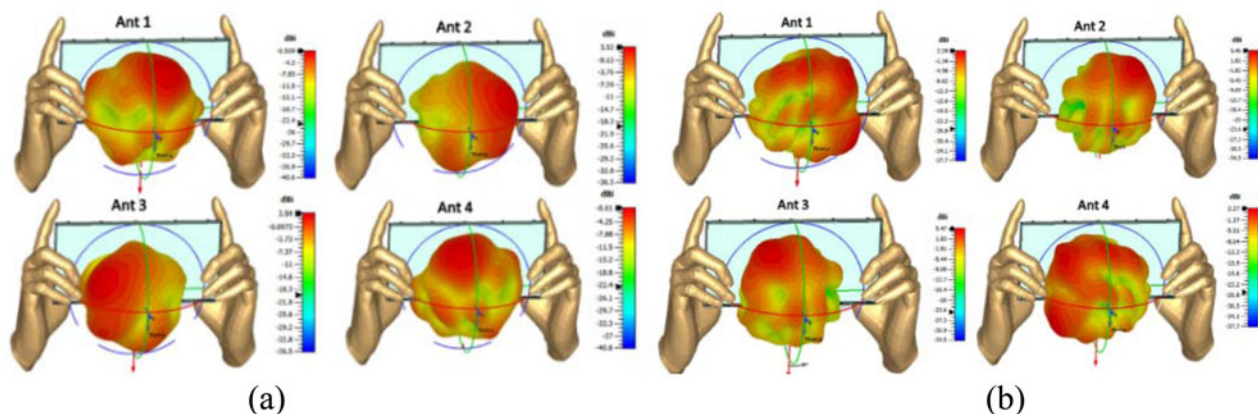


Fig. 18. Simulated 3D radiation pattern of proposed MIMO antenna array in RM usage at (a) 3.5 GHz and (b) 5.5 GHz.

propagation scenario is independent and identically distributed (i.i.d.) Rayleigh-fading channel. It is observed that, the calculated channel capacity is 32, and 38.7 bps/Hz, for 17 and 20 dB SNR in the receiver, respectively, whereas the ideal  $8 \times 8$  MIMO system by assuming zero correlation and 100% efficiency is about 43.96 bps/Hz.

### User's hand effect

To investigate influence of user's hand and head on the performances of the proposed MIMO antenna, two typical configurations, namely, data mode (single-hand usage, DM), and read mode (two-hand usage, RM) are considered. The simulated  $S$  parameters and total efficiency of these modes are shown in Figs 15 and 16. It is observed that for DM scenario shown in Fig. 15(a), the total efficiency of antennas which are close to the phantom hand, i.e., Ant 2, 3, 6, 7 have been reduced more than

that of the other elements, which is reasonable, because the hand tissue is a lossy medium and absorbs some part of radiation power. While efficiency of Ant 1, 4, 5, 8 are still higher than 50 and 60% in the low band and high band, respectively. As shown in Fig. 16(a), in RM case, Ant 5, 8 are fully covered by fingers hand, hence, the efficiency of these elements has become 40% lower than that of the free space scenario.

Also, Ant 1, 4 which are close to the index finger, experience deteriorated efficiency. In this mode, Ant 2, 3, 6, 7 still have efficiency higher than 50 and 60% in the two desired.

Frequency bands. In talk mode configuration, as shown in Fig. 16(a), however, the total efficiencies of all antennas have deteriorated, the efficiency of Ant 2, 3, 6 and 7 are better than 30 and 50% in low band and high band, respectively. The simulated  $S$ -parameters of the proposed MIMO antenna array under three scenarios in vicinity of the user's hand are displayed in Figs 15 (b) and 16(b). As can be seen; however, the resonant frequency

**Table 3** Comparison between the proposed antenna array and the referenced 5G antennas.

References	Bandwidth (GHz)	Efficiency (%)	Isolation (dB)	Decoupling method	Mean effective gain (dBi)	ECC	Peak channel capacity (bps/Hz)
Proposed work	3.4–3.6, 5.15–5.925 (–6 dB)	60–84 (low band), 80–95 (high band)	>10 (low band), >15 (high band)	Pattern diversity	–4.69 to –1.76	<0.15	38.7 (SNR = 20)
[14] <sup>a</sup>	3.4–3.6, 4.8–5.1 (–6 dB)	40–85 (low band), 41–72 (high band)	>11.5	NL	–6 to –5	<0.08	38.5 (SNR = 20)
[15]	3.4–3.6, 5.15–5.925 (–6 dB)	50–56 (low band), 53–65 (high band)	>12	–	NG	<0.1	38.8/39.7 (SNR = 20)
[16]	3.4–3.6 (–10 dB)	60–70	>20	–	NG	<0.01	35 (SNR = 20)
[17]	3.4–3.6 (–10 dB)	55–60	>11	–	–7 to –6.3	<0.1	36 (SNR = 20)
[18]	3.4–3.6 (–6 dB)	40–60	>15	NL and GS	NG	<0.15	35 (SNR = 20)
[19]	3.3–3.9 (–6 dB)	60–70	>15	Orthogonal polarization	NG	<0.01	NG
[25]	3.25–3.65 (–6 dB)	58–72	>12	–	–2.96 to –6.31	<0.1	38.5 (SNR = 20)
[26]	3.3–5, 3.3–4.2 (–6 dB)	45–65	>10	–	–1.26	<0.26	37.8 (SNR = 20)
[27]	3.3–6 (–6 dB)	40–90	>18	Slot element	NG	<0.05	NG
[28]	3.4–3.8, 4.8–5.0	42–83, 40–85	>15.5	Multiple slots	NG	<0.07	37.3–38.3
[29]	3.2–4 (–6 dB)	50–75	>11	Strip elements	NG	<0.005	NG
[30]	3.3–6.4 (–6 dB)	>52	>12	T-shaped strip	NG	<0.08	37.8–40

<sup>a</sup>Only 8 × 8 MIMO array are considered for comparison.

Abbreviations: NL, neutralization line; GS, ground slot; NG, not give.

of 3.5 and 5.5 GHz are slightly deviated, the two desired frequency bands are still fully covered under the impedance matching of –6 dB. Also, as can be seen, isolation is not influenced by the hand and head of user.

To further investigate the impact of user on the radiation characteristics of the proposed MIMO antenna, the 3D radiation pattern of elements is simulated in the circumstance of data mode and read mode at two frequencies 3.5 and 5.5 GHz, that shown in Figs 17 and 18, respectively. Obviously, it is observed that, the characteristics radiation of the antenna has been influenced by the user's hand; however, it is not working with good radiation coverage and sufficient gain values. In conclusion, the proposed MIMO system is suitable in the practical application and can be considered as a good candidate for 5G smartphone.

Table 3 shows the performance comparison between the proposed antenna array and those that have been reported. It is observed that, the proposed eight-element array has higher isolation (>10 and >15 dB in the LB and HB, respectively) with a lesser loss in total efficiency (>60 and >80% in the LB and HB, respectively), which, in [14] and [15], this feature have not been achieved. In addition, multi-band operation antenna which is important in the mobile phone communication, has not been implemented in [5, 16–18]. Therefore, it can be concluded that, the proposed antenna array can support dual-band operation with high total efficiency and isolation, which is a unique feature that all the references do not have.

## Conclusion

In this paper, a dual-band eight-elements MIMO antenna array for 5G future mobile phone operating in the 3.5 GHz (3.4–3.6

GHz) and 5.5 GHz (5.15–5.925 GHz) for 5G future mobile phone has been presented, fabricated and measured. In particular, the antenna elements include a comb-shaped monopole antenna and L-shaped open slot antenna that are located on the frame of handset. Two desired frequencies bands have been fully covered under the impedance matching of –6 dB and high isolation better than 11.5 and 15 dB has been achieved without any decoupling structure. The simulated total efficiency is better than 60 and 80% in the low band and high band, respectively. Due to proper placement of the antenna elements, pattern diversity has been achieved which improves the ECC between antenna elements (ECC < 0.1). Furthermore, the calculated channel capacity by considering impact of the total efficiency is 38.7 bps/Hz (SNR = 20 dB). The performances of proposed antenna in vicinity of user's hand have also been investigated and the results indicated that the proposed MIMO antenna can be considered as a good candidate for 5G smartphone.

## References

1. Al-Hadi AA, Ilvonen J, Valkonen R and Viikari V (2014) Eight-element antenna array for diversity and MIMO mobile terminal in LTE 3500 MHz band. *Microwave and Optical Technology Letters* **56**, 1323–1327.
2. Wong K-L, Kang T-W and Tu M-F (2011) Internal mobile phone antenna array for LTE/WWAN and LTE MIMO operations. *Microwave and Optical Technology Letters* **53**, 1569–1573.
3. Jensen MA and Wallace JW (2004) A review of antennas and propagation for MIMO wireless communications. *IEEE Transactions on Antennas and Propagation* **52**, 2810–2824.
4. WRC-15 Press Release (2015) World Radiocommunication Conference allocates spectrum for future innovation, [Online]. Available: <http://>

- [www.itu.int/net/pressoffice/press\\_releases/2015/56.aspx#.XOOHXth9JIU](http://www.itu.int/net/pressoffice/press_releases/2015/56.aspx#.XOOHXth9JIU), Nov. 27, 2015.
5. **Jiang W, Liu B, Cui Y and Hu W** (2019) High-isolation eight-element MIMO array for 5G smartphone applications. *IEEE Access* **7**, 2169–3536.
  6. **Wong K-L, Lu J-Y, Chen L-Y, Li W-Y and Ban Y-L** (2016) 8-antenna and 16-antenna arrays using the quad-antenna linear array as a building block for the 3.5 GHz LTE MIMO operation in the smartphone. *Microwave and Optical Technology Letters* **58**, 174–181.
  7. **Li Y, Sim C-Y-D, Luo Y and Yang G** (2019) Metal-frame-integrated eight-element multiple-input multiple-output antenna array in the long term evolution bands 41/42/43 for fifth generation smartphones. *The International Journal of RF and Microwave Computer-Aided Engineering* **29**, e21495.
  8. **Zhao HX, Yeo SP and Ong LC** (2018) Decoupling of inverted-F antennas with high-order modes of ground plane for 5G mobile MIMO platform. *IEEE Transactions on Antennas and Propagation* **66**, 4485–4495.
  9. **Li M-Y, Ban Y-L, Xu Z-Q, Wu G, Kang K and Yu Z-F** (2016) Eight-port orthogonally dual-polarized antenna array for 5G smartphone applications. *IEEE Transactions on Antennas and Propagation* **64**, 3820–3830.
  10. **Li M-Y, Xu Z-Q, Ban Y-L, Sim C-Y-D and Yu Z-F** (2017) Eight-port orthogonally dual-polarised MIMO antennas using loop structures for 5G smartphone, IET microwe. *Antennas Propag* **11**, 1810–1816.
  11. **Li MY, Ban YL, Xu ZQ, Guo J and Yu ZF** (2018) Tri-polarized 12-antenna MIMO array for future 5G smartphone applications. *IEEE Access* **6**, 6160–6170.
  12. **Ding CF, Zhang XY, Xue C-D and Sim C-Y-D** (2018) Novel pattern diversity-based decoupling method and its application to multielement MIMO antennas. *IEEE Transactions on Antennas and Propagation* **66**, 4976–4985.
  13. **Xu H, Zhou H, Gao S, Wang H and Cheng Y** (2017) Multimode decoupling technique with independent tuning characteristic for mobile terminals. *IEEE Transactions on Antennas and Propagation* **65**, 6739–6751.
  14. **Guo J, Cui L, Li C and Sun B** (2018) Side-edge frame printed eight-port dual-band antenna array for 5G smartphone applications. *IEEE Transactions on Antennas and Propagation* **66**, 7412–7417.
  15. **Zou H, Li Y, Sim C-Y-D and Yang G** (2018) Design of 8 × 8 dual-band MIMO antenna array for 5G smartphone applications. *International Journal of RF and Microwave Computer-Aided Engineering* **9**, 21420.
  16. **Anping Zhao ZR** (2019) Size reduction of self-isolated MIMO antenna system for 5G Mobile phone applications. *IEEE Antennas and Wireless Propagation Letters* **18**, 152–156.
  17. **Wong K-L, Tsai C-Y and Lu J-Y** (2017) Two asymmetrically mirrored gap-coupled loop antennas as a compact building block for eight-antenna MIMO array in the future smartphone. *IEEE Transactions on Antennas and Propagation* **65**, 1765–1778.
  18. **Jiang W, Liu B, Cui Y and Hu W** (2019) High-isolation eight-element MIMO array for 5G smartphone applications. *IEEE Access* **7**, 34104–34112.
  19. **Parchin NO, Al-Yasir Y-I, Ali A-H, Elfergani I, Noras J-M, Rodriguez J and Abd-Alhameed R-A** (2019) Eight-element dual-polarized MIMO slot antenna system for 5G smartphone applications. *IEEE Access* **7**, 15612–15622.
  20. **Taga T** (1990) Analysis for mean effective gain of mobile antennas in land mobile radio environments. *IEEE Transactions on Vehicular Technology* **2**, 117–131.
  21. **Sharawi MS** (2013) Printed multi-band MIMO antenna systems and their performance metrics. *IEEE Antennas and Propagation Magazine* **55**, 218–232.
  22. **Tian R, Lau BK and Ying Z** (2011) Multiplexing efficiency of MIMO antennas. *IEEE Antennas and Wireless Propagation Letters* **10**, 183–186.
  23. **Li Z, Du Z, Takahashi M, Saito K and Ito K** (2011) Reducing mutual coupling of MIMO antennas with parasitic elements for mobile terminals. *IEEE Transactions on Antennas and Propagation* **60**, 473–481.
  24. **Yun JX and Vaughan RG** (2011) Multiple element antenna efficiency and its impact on diversity and capacity. *IEEE Transactions on Antennas and Propagation* **60**, 529–539.
  25. **Kiani SH, Altaf A, Abdullah M, Muhammad F, Shoaib N, Anjum M-R, Damaševičius R and Blažauskas T** (2020) Eight element side edged framed MIMO antenna array for future 5G smart phones. *Micromachines* **11**, 956.
  26. **Guo L, Liu Z, Liu H, Huang D and Du Z** (2020) Wideband eight-element antenna for 5G metal frame mobile phone applications. *International Journal of RF and Microwave Computer-Aided Engineering* **30**, 22442.
  27. **Yuan XT, He W, Hong KD, Han CZ, Chen Z and Yuan T** (2020) Ultra-wideband MIMO antenna system with high element-isolation for 5G smartphone application. *IEEE Access* **8**, 56281–56289.
  28. **Hu W, Qian L, Gao S, Wen L-H, Luo Q, Xu H, Liu X, Liu Y and Wang W** (2019) Dual-band eight-element MIMO array using multi-slot decoupling technique for 5G terminals. *IEEE Access* **7**, 153910–153920.
  29. **Parchin NO, Basherlou H, Jahanbakhsh AY, Yasir IA and Abd-Alhameed RA** (2020) A broadband multiple-input multiple-output loop antenna array for 5G cellular communications. *International Journal of Electronics and Communications* **127**, 153476.
  30. **Wang H, Zhang R, Luo Y and Yang G** (2020) Design of MIMO antenna system operating in wideband of 3300 to 6400 MHz for future 5G mobile terminal applications. *International Journal of RF and Microwave Computer-Aided Engineering* **30**, 22426.



**Mahsa Zabetiakhmal** obtained the B.Sc. and M.Sc. both in electrical communications from the Department of Electrical Engineering at Amirkabir University of Technology (Tehran Polytechnic), Tehran, Iran in 2017 and 2019, respectively. She is currently a Ph.D. student in Amirkabir University of Technology. Her research fields are planar structure, antennas, and 5G systems.



**Gholamreza Moradi** (M'09–SM'16) obtained the Ph.D. degree in electrical engineering from Amirkabir University of Technology (Tehran Polytechnic), Tehran, Iran in 2002. He is currently an associate professor in the Electrical Engineering Department, Amirkabir University of Technology, and director of microwave measurement research lab. From June 2016 to February 2017, he was a visiting professor with the University of Alberta. He has published and presented over 100 papers in the refereed journals and international conferences. His main research interests are numerical electromagnetics, antennas, active microwave and mm-wave circuits and systems.



**Ayaz Ghorbani** obtained the postgraduate diploma, M.Phil., and Ph.D. degrees in electrical and communication engineering and the Ph.D. degree from the University of Bradford, Bradford, UK, in 1984, 1985, 1987, and 2004, respectively. Since 1987, he has been teaching various courses with the Department of Electrical Engineering, Amirkabir University of Technology, Tehran, Iran. He has authored or co-authored more than 100 papers in various conferences as well as journals. Dr. Ghorbani obtained the John Robertshaw Travel Award and the URSI Young Scientists Award from the General Assembly of URSI, Prague, Czech Republic, in 1990. He was a recipient of the Seventh and Tenth Khwarazmi International Festival Prizes, in 1993 and 1995, respectively, for design and implementation of an anti-echo chamber and microwave subsystems.